Signal Processing 89 (2009) 1678–1682

Contents lists available at ScienceDirect

Signal Processing

journal homepage: www.elsevier.com/locate/sigpro

Fast communication

Route to chaos in a third-order phase-locked loop network

L.H.A. Monteiro [a,b,*], A.C. Lisboa [b], M. Eisencraft [a,b]

[a] Universidade Presbiteriana Mackenzie, Escola de Engenharia, Pós-graduação em Engenharia Elétrica, Rua da Consolação, n. 896, CEP 01302-907, São Paulo, SP, Brazil

[b] Universidade de São Paulo, Escola Politécnica, Departamento de Engenharia de Telecomunicações e Controle, Av. Prof. Luciano Gualberto, travessa 3, n. 380, CEP 05508-900, São Paulo, SP, Brazil

ARTICLE INFO

Article history:
Received 24 November 2008
Received in revised form
12 February 2009
Accepted 5 March 2009
Available online 14 March 2009

Keywords:
Chaos
Hopf bifurcation
Period-doubling bifurcation
Phase-locked loop
Saddle–saddle bifurcation
Synchronism

ABSTRACT

Phase-locked loops (PLLs) are widely used in applications related to control systems and telecommunication networks. Here we show that a single-chain master–slave network of third-order PLLs can exhibit stationary, periodic and chaotic behaviors, when the value of a single parameter is varied. Hopf, period-doubling and saddle–saddle bifurcations are found. Chaos appears in dissipative and non-dissipative conditions. Thus, chaotic behaviors with distinct dynamical features can be generated. A way of encoding binary messages using such a chaos-based communication system is suggested.

1. Introduction

Phase-locked loop (PLL) is an electronic device designed to extract time signals from transmission channels. This device has been extensively employed in applications requiring automatic control of frequency with the aim of obtaining synchronism, such as in computers, modems, motors, radars, radio and television receivers, telecommunication networks, etc. (e.g. [1,2]). It is a closed loop composed by three elements: a phase detector (PD), a low-pass filter (LPF) and a voltage controlled oscillator (VCO), as illustrated in Fig. 1.

Consider a single-chain master–slave telecommunication network, where each node sends signals to a unique neighboring node. Let $\theta_{i(j)}(t)$ be the phase of the input signal and $\theta_{o(j)}(t)$ the phase of the output signal of the j-th PLL. The role of j-th PLL is to synchronize the signal $v_{o(j)}(t)$ generated by its own VCO with the signal $v_{i(j)} = v_{o(j-1)}(t)$ provided by VCO of the $(j-1)$-th PLL $(j = 1, 2, \ldots)$.

Assume that:

$$v_{o(j)}(t) = V_{o(j)} \cos\left[\omega_0 t + \theta_{o(j)}(t) + (j-1)\frac{\pi}{2}\right] \tag{1}$$

for $j = 0, 1, 2, \ldots$. Thus, the output signal of every VCO has periodic form with central frequency ω_0 and amplitude $V_{o(j)} > 0$. The index $j = 0$ labels the master clock.

The adjustable phase of the output signal of j-th PLL is $\theta_{o(j)}(t)$ and it depends on the time-varying phase $\theta_{i(j)}(t)$ of the input signal. A synchronous solution corresponds to the phase errors defined by $\phi_j(t) \equiv \theta_{i(j)}(t) - \theta_{o(j)}(t) = \theta_{o(j-1)}(t) - \theta_{o(j)}(t)$ $(j = 1, 2, \ldots)$ assuming constant values or, equivalently, the frequency errors $d\phi_j(t)/dt \equiv w_j(t) = d\theta_{i(j)}(t)/dt - d\theta_{o(j)}(t)/dt = d\theta_{o(j-1)}(t)/dt - d\theta_{o(j)}(t)/dt$ vanishing (e.g. [3–6]).

We consider that the input–output relation concerning the LPF of the j-th PLL is described by the second-order differential equation:

$$\frac{d^2 v_{c(j)}(t)}{dt^2} + k_j \frac{dv_{c(j)}(t)}{dt} + v_{c(j)}(t) = \frac{dv_{d(j)}(t)}{dt} + v_{d(j)}(t) \tag{2}$$

* Corresponding author at: Universidade Presbiteriana Mackenzie, Escola de Engenharia, Pós-graduação em Engenharia Elétrica, Rua da Consolação, n. 896, CEP 01302-907, São Paulo, SP, Brazil.
E-mail addresses: luizm@mackenzie.br, luizm@usp.br (L.H.A. Monteiro).

0165-1684/$ - see front matter © 2009 Elsevier B.V. All rights reserved.
doi:10.1016/j.sigpro.2009.03.006

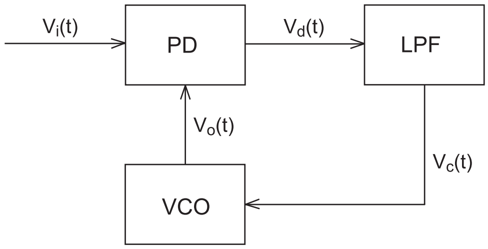

Fig. 1. Block diagram of a PLL. The PLL input signal is represented by $v_i(t)$, the VCO output signal by $v_o(t)$, the PD output signal by $v_d(t)$ and the LPF output signal by $v_c(t)$.

where $v_{d(j)}(t)$ is the input and $v_{c(j)}(t)$ is the output of the LPF, and $k_j \geqslant 0$. PLLs with similar filters were already studied (e.g. [4,7,8]).

Here all PLLs use signal multiplier as PD; therefore, the PD output $v_{d(j)}(t)$ is given by:

$$v_{d(j)}(t) = k_{d(j)} v_{i(j)}(t) v_{o(j)}(t) = k_{d(j)} v_{o(j-1)}(t) v_{o(j)}(t) \tag{3}$$

where $k_{d(j)} > 0$ is the PD gain of the j-th PLL.

The VCO output phase $\theta_{o(j)}(t)$ is controlled by the signal $v_{c(j)}(t)$ according to:

$$\frac{d\theta_{o(j)}(t)}{dt} = k_{v(j)} v_{c(j)}(t) \tag{4}$$

where $k_{v(j)} > 0$ is the VCO gain of the j-th PLL.

It is a common approximation to consider that the second-harmonic appearing in $v_{d(j)}(t)$ will be cut out by the filter (for a discussion, see [3,5]). Thus, the expression for $v_{d(j)}(t)$ can be reduced to:

$$v_{d(j)}(t) \simeq \frac{k_{d(j)} V_{o(j)} V_{o(j-1)}}{2} \sin \phi_j(t) \tag{5}$$

By combining the expressions (1)–(5), the dynamics of the j-th PLL is described by the following nonlinear ordinary differential equation:

$$\frac{d^3\phi_j(t)}{dt^3} + k_j \frac{d^2\phi_j(t)}{dt^2} + (1 + \mu_j \cos\phi_j(t)) \frac{d\phi_j}{dt} + \mu_j \sin\phi_j(t)$$
$$= \frac{d^3\theta_{i(j)}(t)}{dt^3} + k_j \frac{d^2\theta_{i(j)}(t)}{dt^2} + \frac{d\theta_{i(j)}(t)}{dt} \equiv g_j(t) \tag{6}$$

where $\mu_j \equiv (V_{o(j)} V_{o(j-1)} k_{d(j)} k_{v(j)})/2 > 0$ is called PLL gain.

Since 1980s chaotic circuits (e.g. [9,10]) have been theoretically analyzed and physically built in order to be used in applications involving cryptography (e.g. [11,12]), image processing (e.g. [13]), modulation (e.g. [11,12]), network synchronization (e.g. [14]), pseudo-random number generation (e.g. [11,12]), etc. Here we analytically and numerically investigate the asymptotical solutions of the network described by Eq. (6) and propose a way of encoding binary messages using the chaotic behaviors appearing in such a network. Analyses for first-order (e.g. [15–17]), second-order (e.g. [18,19]), and different third-order PLL networks (e.g. [4,6,8,20]) can be found in the literature.

2. Analysis

Firstly, consider the case where there are two nodes; that is, only one slave ($j = 1$) linked to the master clock ($j = 0$). Assume that the master phase $\theta_{o(0)}(t)$ presents a linear variation with the time, that is: $\theta_{o(0)}(t) = \Omega t + c$, with $\Omega \geqslant 0$ and $c =$ constant. Observe that when $\theta_{o(0)}(t) \equiv \theta_{i(1)}(t)$ varies as a ramp input ($\Omega \neq 0$), then $g_1(t) = \Omega$ becomes a step input.

The third-order differential Eq. (6) for $\phi_1(t) \equiv \theta_{o(0)}(t) - \theta_{o(1)}(t)$ can be rewritten as the following three first-order differential equations:

$$\frac{d\phi_1(t)}{dt} \equiv w_1(t) \equiv f_1(\phi_1, w_1, a_1)$$
$$\frac{dw_1(t)}{dt} \equiv a_1(t) \equiv f_2(\phi_1, w_1, a_1)$$

$$\frac{da_1(t)}{dt} = -k_1 a_1(t) - (1 + \mu_1 \cos\phi_1(t)) w_1(t) - \mu_1 \sin\phi_1(t)$$
$$+ \Omega \equiv f_3(\phi_1, w_1, a_1) \tag{7}$$

Notice that $\vec{\nabla}\cdot\vec{f}(\phi_1, w_1, a_1) = -k_1$, where $\vec{f} = (f_1, f_2, f_3)$. Thus, the divergent of the vector field $\vec{f}$ related to the system (7) is negative for $k_1 > 0$, implying that the system is dissipative (which means that volumes in the state space $\phi_1 \times w_1 \times a_1$ contract along the flow). For $k_1 = 0$ such a divergent is null; hence, this system is conservative (which means that volumes in the state space are preserved).

In the PLL jargon, the capture range is defined as the set of values of the velocity Ω such that the closed loop is able of reaching a synchronous state. This state corresponds to a stationary solution with $\phi_1(t) = \phi_1^* =$ constant, $w_1(t) = w_1^* = 0$, $a_1(t) = a_1^* = 0$ and is represented by the equilibrium point $(\phi_1^*, 0, 0)$ in the state space.

The nonlinear system (7) presents two equilibrium points: a point with $\phi_{1a}^* = \arcsin(\Omega/\mu_1)$ $(0 \leqslant \phi_{1a}^* \leqslant \pi/2)$ and another point with $\phi_{1b}^* = \pi - \arcsin(\Omega/\mu_1)$ $(\pi/2 \leqslant \phi_{1b}^* \leqslant \pi)$. These points exist only if $0 \leqslant \Omega/\mu_1 \leqslant 1$. When $\Omega/\mu_1 > 1$, there is not synchronism.

The local stability of $(\phi_{1a}^*, 0, 0)$ and $(\phi_{1b}^*, 0, 0)$ is determined from the eigenvalues $\lambda_{1,2,3}$ of the Jacobian matrix related to the system (7) linearized around each point. Hartman–Grobman Theorem states that an equilibrium point is locally asymptotically stable when all eigenvalues have negative real parts (e.g. [21]). For the system (7), the eigenvalues $\lambda_{1,2,3}$ are the roots of the characteristic equation:

$$\lambda^3 + a_1\lambda^2 + a_2\lambda + a_3 = 0 \tag{8}$$

where $a_1 = k_1$, $a_2 = 1 + \mu_1 \cos\phi_1^*$ and $a_3 = \mu_1 \cos\phi_1^*$. According to Routh–Hurwitz Criterion (e.g. [22]), all eigenvalues have negative real parts if $a_1 > 0$, $a_2 > 0$, $a_3 > 0$ and $a_1 a_2 > a_3$. Here, this last condition corresponds to:

$$k_1 > k_{c1} \equiv \frac{\mu_1 \cos\phi_1^*}{1 + \mu_1 \cos\phi_1^*} \tag{9}$$

Therefore, for $k_1 = 0$, both equilibrium points are unstable and there is a subcritical saddle–saddle bifurcation for $\Omega/\mu_1 = 1$, because if $\Omega/\mu_1 < 1 - \varepsilon$ for $\varepsilon \to 0_+$ there are two unstable equilibrium points, and if $\Omega/\mu_1 > 1 + \varepsilon$ there are not equilibrium points. For $k_1 > 0$ and $0 \leqslant \Omega/\mu_1 < 1$, ϕ^*_{1b} is unstable (because $\cos\phi^*_{1b} < 0$) and ϕ^*_{1a} is an asymptotically stable synchronous state only if $k_1 > k_{c1}$. For $k_1 = k_{c1}$, ϕ^*_{1a} suffers a supercritical Hopf bifurcation (e.g. [21]). For this critical value of k_1, $\lambda_{1,2} = \pm i\sigma$ are imaginary numbers ($\sigma > 0$) and λ_3 is a negative real number. For $k_1 < k_{c1}$, ϕ^*_{1a} becomes an unstable equilibrium point and an asymptotically stable limit-cycle appears in the state space $\phi_1 \times w_1 \times a_1$. Hence, the phase error $\phi_1(t)$ periodically oscillates if $k_1 < k_{c1}$. For $k_1 \lesssim k_{c1}$, the oscillation period T is given by $T \simeq 2\pi/\sigma \simeq 2\pi/(\sqrt{1 + \mu_1 \cos\phi^*_{1a}})$.

For $k_1 = 0$, it is numerically found that the system can exhibit sensitive dependence on initial conditions (SDIC), characterized by the existence of a positive Lyapunov exponent (implying exponential divergence of two neighboring trajectories in the state space, e.g. [21]). Thus, there can be chaotic behavior but there is no (chaotic) attractor because the system is conservative.

For instance, for $\mu_1 = 1$ and $\Omega = 0.95$, then $\phi^*_{1a} \simeq 1.253$; consequently, $k_{c1} \simeq 0.238$ (from expression (9)). Figs. 2 and 3 present the time evolutions of $a_1(t)$ obtained by employing the fourth-order Runge–Kutta integration method with time step of 0.01 for solving the differential equations (7). There are three distinct situations: $k_1 = 0$ (chaos without attractor), $k_1 = 0.2$ (the attractor is a limit-cycle; notice in Fig. 3 that the oscillation period is about $T \simeq 5.5$) and $k_1 = 0.4$ (the attractor is an equilibrium point with $a^*_1 = 0$). Observe that Fig. 2 illustrates the SDIC phenomenon.

For $0 < k_1 < k_{c1}$, numerical simulations reveal that two Lyapunov exponents are negative and the other is null; therefore, the asymptotical solutions correspond to stable limit-cycles. Moreover, for k varying from k_{c1} to zero there occurs a cascade of period-doubling bifurcations (e.g. [21]) as shown in Fig. 4. If $\mu_1 = 1$ and $\Omega = 0.95$, then there is a period-1 limit-cycle for $0.048 \lesssim k_1 \lesssim 0.238$; a period-2 limit-cycle for $0.032 \lesssim k_1 \lesssim 0.047$; a period-4 limit-cycle for $0.030 \lesssim k_1 \lesssim 0.031$ and so on. For $k_1 = 0$, the values of the three Lyapunov exponents are $L_1 = -L_2 \simeq 0.05$ and $L_3 = 0$. Observe that the system is conservative in such a case; hence, $L_1 + L_2 + L_3 = 0$. Thus, there is chaos but no attractor. The values of the Lyapunov exponents $L_{1,2,3}$ related to this system were calculated by using the algorithm proposed by Wolf et al. [23].

Now, consider a three-node single-chain network, with a master clock plus two PLL slaves. In this case, the differential equations for the second slave are:

$$\frac{d\phi_2(t)}{dt} \equiv w_2(t)$$
$$\frac{dw_2(t)}{dt} \equiv a_2(t)$$

$$\frac{da_2(t)}{dt} = -k_2 a_2(t) - (1 + \mu_2 \cos\phi_2(t))w_2(t) - \mu_2 \sin\phi_2(t) + \mu_1(\cos\phi_1(t))w_1 + \mu_1 \sin\phi_1(t) \quad (10)$$

where $\phi_2(t) \equiv \theta_{o(1)}(t) - \theta_{o(2)}(t)$.

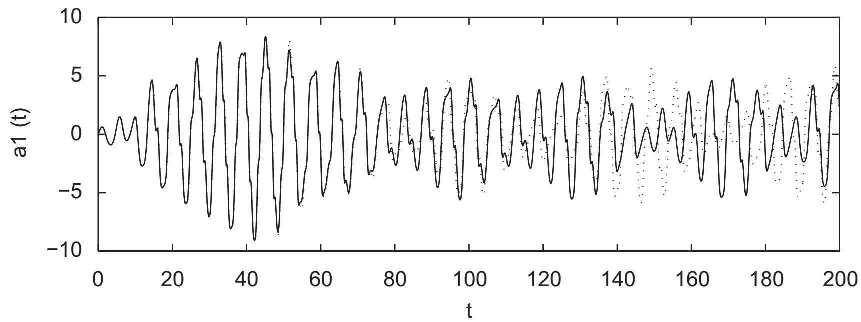

Fig. 2. Time evolutions of $a_1(t)$ for $\Omega = 0.95$, $\mu_1 = 1$ and $k = 0$. Solid line: initial condition is $(\phi_1(0), w_1(0), a_1(0)) = (0, 0, 0)$; dotted line: initial condition is $(\phi_1(0), w_1(0), a_1(0)) = (0.01, 0, 0)$.

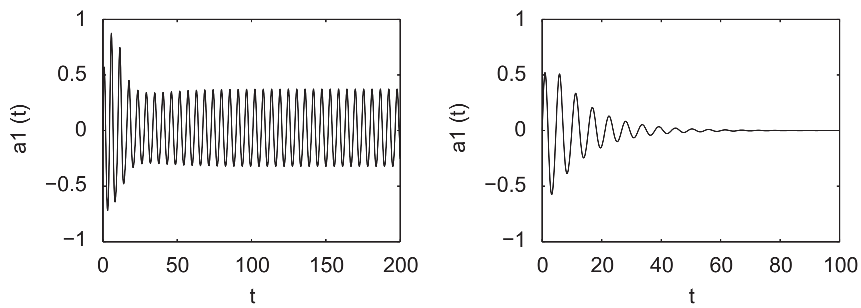

Fig. 3. Time evolutions of $a_1(t)$ for $\Omega = 0.95$ and $\mu_1 = 1$. Left: $k_1 = 0.2$; right: $k_1 = 0.4$. Initial condition: the origin of the state space.

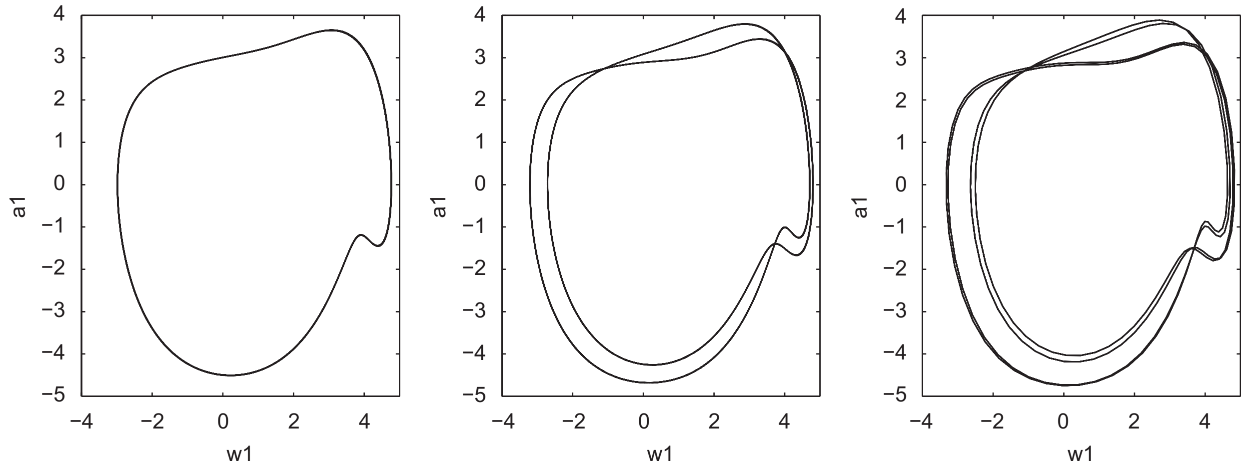

Fig. 4. Attractor projected onto the plane $w_1 \times a_1$. Left: 1-period limit-cycle for $k = 0.05$; centre: 2-period limit-cycle for $k = 0.04$; right: 4-period limit-cycle for $k = 0.03$. The number of the period corresponds to the number of intersections between the closed curve and the semi-axis defined by $w_1 = 0$ and $a_1 > 0$.

The system composed by the Eqs. (7) and (10) presents synchronous solution given by $(\phi_1^*, w_1^*, a_1^*, \phi_2^*, w_2^*, a_2^*) = (\arcsin(\Omega/\mu_1), 0, 0, \arcsin(\Omega/\mu_2), 0, 0)$ only if $0 \leqslant \Omega/\mu_j \leqslant 1$ for $j = 1, 2$. By inspecting the characteristic equation of such a system, then an equilibrium point is locally asymptotically stable only if $k_j > 0$, $\cos\phi_j^* > 0$ and $k_j > k_{cj} \equiv (\mu_j \cos\phi_j^*)/(1 + \mu_j \cos\phi_j^*)$ for $j = 1, 2$. Saddle–saddle bifurcations occur for $\Omega/\mu_j = 1$ and Hopf bifurcations for $k_j = k_{cj}$ for $j = 1, 2$. Thus, if $k_1 > k_{c1}$ and $k_2 > k_{c2}$, then both PLLs tend to a synchronous (stationary) solution (if it exists, of course). If $k_1 > k_{c1}$ and $k_2 < k_{c2}$, then the PLL-1 tends to a stationary solution and the PLL-2 to a limit-cycle; and if k_2 is varied from k_{c2} to zero there occurs a cascade of period-doubling bifurcations as already mentioned. If $k_1 < k_{c1}$, numerical simulations indicate that both PLLs tend to a limit-cycle; in this case, five Lyapunov exponents are negative and the sixth is null. If $k_1 = 0$ or $k_2 = 0$, then $L_1 = -L_2 > 0$, $L_3 = 0$ and $L_{4,5,6} < 0$; the system is dissipative in such a situation; hence, there is a chaotic attractor in the six-dimensional state space. If $k_1 = k_2 = 0$, the system is conservative and $L_1 = -L_2 > 0$, $L_3 = -L_4 > 0$ and $L_5 = L_6 = 0$ (for instance, for $\Omega = 0.95$ and $\mu_1 = \mu_2 = 1$, then $L_1 \simeq 0.06$ and $L_3 \simeq 0.02$); thus, there is non-dissipative chaos.

If there are n slaves, the condition for existing synchronism along the single-chain network is $0 \leqslant \Omega/\mu_j \leqslant 1$ and this solution is asymptotically stable only if $k_j > 0$, $\cos\phi_j^* > 0$ and $k_j > k_{cj} \equiv (\mu_j \cos\phi_j^*)/(1 + \mu_j \cos\phi_j^*)$ for $j = 1, 2, \ldots, n$. Saddle–saddle, Hopf and period-doubling bifurcations can be produced in a similar way as showed for $n = 1$ and $n = 2$. For any value of n, the system is conservative if $k_j = 0$ for all values of j, and dissipative if $k_j > 0$ for any j. Again, conservative and dissipative chaos can be generated by such a PLL network.

3. Conclusion

We analytically and numerically investigated the asymptotical behaviors of a third-order PLL network. We derived conditions for generating stable synchronism, periodic and chaotic solutions. Chaos can be produced in conservative and dissipative conditions. For instance, with a three-node network (when there is one master clock and two slaves), dissipative chaos can be achieved by setting $k_1 = 0$ and $k_2 > 0$ or vice versa; and conservative chaos occurs for $k_1 = k_2 = 0$. Hence, by controlling the values of k_1 and k_2, chaotic waveforms with distinct dynamical features can be produced, which be used for encoding information in a chaos-based communication system. Thus, this three-node network can be employed as a binary chaos shift keying transmitter (e.g. [11,12,24]). In fact, by fixing $k_1 = 0$, binary messages can be generated by switching k_2 between 0 and $K > 0$. When $k_2 = 0$, the transmitted symbol is related to a chaotic time series where the sum of the Lyapunov exponents is null; when $k_2 = K$, the other symbol concerns a chaotic time series where such a sum is negative. Then, by estimating the sum of the Lyapunov exponents, a transmitted symbol can be detected in the receiver and the original message can be recovered. A natural extension of this work is to implement this kind of encoding and to explore other ways of encoding information by using three or more PLL slaves.

Acknowledgment

LHAM is partially supported by CNPq; ACL was supported by CNPq.

References

[1] R.E. Best, Phase-locked Loops: Design, Simulation, and Applications, McGraw-Hill, New York, 2003.
[2] F.M. Gardner, Phaselock Techniques, Wiley, New York, 2005.
[3] J.R.C. Piqueira, L.H.A. Monteiro, Considering second-harmonic terms in the operation of the phase detector for second-order phase-locked loop, IEEE Transactions on Circuits and Systems I 50 (6) (2003) 805–809.
[4] L.H.A. Monteiro, D.N. Favaretto Filho, J.R.C. Piqueira, Bifurcation analysis for third-order phase-locked loops, IEEE Signal Processing Letters 11 (5) (2004) 494–496.

[5] J.R.C. Piqueira, E.Y. Takada, L.H.A. Monteiro, Analyzing the effect of the phase-jitter in the operation of second-order phase-locked loops, IEEE Transactions on Circuits and Systems II 52 (6) (2005) 331–335.
[6] J.R.C. Piqueira, L.H.A. Monteiro, All-pole phase locked-loops: calculating lock-in range by using Evan's root-locus, International Journal of Control 79 (7) (2006) 822–829.
[7] K. Watada, T. Endo, H. Seishi, Shilnikov orbits in an autonomous third-order chaotic phase-locked loop, IEEE Transactions on Circuits and Systems I 45 (9) (1998) 979–983.
[8] B.A. Harb, A.M. Harb, Chaos and bifurcation in a third-order phase locked loop, Chaos, Solitons and Fractals 19 (3) (2004) 667–672.
[9] T. Matsumoto, A chaotic attractor from Chua's circuit, IEEE Transactions on Circuits and Systems 31 (12) (1984) 1055–1058.
[10] T. Endo, L.O. Chua, Chaos from phase-locked loops, IEEE Transactions on Circuits and Systems 35 (8) (1988) 987–1003.
[11] M.P. Kennedy, R. Rovatti, G. Setti (Eds.), Chaotic Electronics in Telecommunications, CRC Press, Boca Raton (Florida), 2000.
[12] L.E. Larson, J.M. Liu, L.S. Tsimring (Eds.), Digital Communications Using Chaos and Nonlinear Dynamics, Springer, New York, 2006.
[13] Y. J. Zhang (Ed.), Advances in Image and Video Segmentation, Springer, New York, 2006.
[14] C.W. Wu, Synchronization in Coupled Chaotic Circuits and Systems, World Scientific, New Jersey, 2002.
[15] L.H.A. Monteiro, R.V. Santos, J.R.C. Piqueira, Estimating the critical number of slaves nodes in a single-chain PLL network, IEEE Communications Letters 7 (9) (2003) 449–450.
[16] L.H.A. Monteiro, N.C.F. Canto, J.G. Chauí-Berlinck, F.M. Orsatti, J.R.C. Piqueira, Global and partial synchronism in phase-locked loop networks, IEEE Transactions on Neural Networks 14 (6) (2003) 1572–1575.
[17] M.K.S. Kunyosi, L.H.A. Monteiro, Recognition of Noisy Images by PLL Networks, Signal Processing 89 (7) (2009) 1311–1319.
[18] J.R.C. Piqueira, C.N. Marmo, L.H.A. Monteiro, Using central manifold theorem in the analysis of master–slave synchronization networks, Journal of Communications and Networks 6 (3) (2004) 1–6.
[19] J.R.C. Piqueira, S.A. Castillo-Vargas, L.H.A. Monteiro, Two-way master–slave double-chain networks: limitations imposed by linear master drift for second-order PLLs as slave nodes, IEEE Communications Letters 9 (9) (2005) 829–831.
[20] J.R.C. Piqueira, M.C. Freschi, Comparing lock-in ranges and transient responses of second- and third-order phase-locked loops in master–slave clock distribution networks, AEU International Journal of Electronics and Communications 62 (6) (2008) 459–463.
[21] J. Guckenheimer, P. Holmes, Nonlinear Oscillations, Dynamical Systems, and Bifurcations of Vector Fields, Springer, New York, 2002.
[22] K. Ogata, Modern Control Engineering, Prentice-Hall, New York, 2001.
[23] A. Wolf, J.B. Swift, H.L. Swinney, J.A. Vastano, Determining Lyapunov exponents from a time series, Physica D 16 (3) (1985) 285–317.
[24] M.P. Kennedy, G. Kolumbán, Digital communication using chaos, Signal Processing 80 (7) (2000) 1307–1320.